1. ORIGINATING ACTIVITY (Corporate author)
Aerospace Medical Research Laboratory
Aerospace Medical Div, Air Force Systems Command
Wright-Patterson Air Force Base, Ohio 45433

2a. REPORT SECURITY CLASSIFICATION
Unclassified

2b. GROUP
N/A

3. REPORT TITLE

ON SOME GEOMETRIC PROPERTIES OF HUMAN RIBS - I

4. DESCRIPTIVE NOTES (Type of report and inclusive dates)

5. AUTHOR(S) (First name, middle initial, last name)
Sanford B. Roberts and Ping Heng Chen

6. REPORT DATE
December 1971

7a. TOTAL NO. OF PAGES
26

7b. NO. OF REFS

8a. CONTRACT OR GRANT NO.

b. PROJECT NO. 7231

c.

d.

9a. ORIGINATOR'S REPORT NUMBER(S)
AMRL-TR-71-29
Paper No 13

9b. OTHER REPORT NO(S) (Any other numbers that may be assigned this report)

10. DISTRIBUTION STATEMENT

Approved for public release; distribution unlimited

11. SUPPLEMENTARY NOTES

12. SPONSORING MILITARY ACTIVITY
Aerospace Medical Research Laboratory
Aerospace Medical Div, Air Force Systems Command, Wright-Patterson AFB, OH 45433

13. ABSTRACT

The Symposium on Biodynamics Models and Their Applications took place in Dayton, Ohio, on 26-28 October 1970 under the sponsorship of the National Academy of Sciences - National Research Council, Committee on Hearing, Bioacoustics, and Biomechanics; the National Aeronautics and Space Administration; and the Aerospace Medical Research Laboratory, Aerospace Medical Division, United States Air Force. Most technical areas discussed included application of biodynamic models for the establishment of environmental exposure limits, models for interpretation of animal, dummy, and operational experiments, mechanical characterization of living tissue and isolated organs, models to describe man's response to impact, blast, and acoustic energy, and performance in biodynamic environments.

26

DD FORM 1 NOV 1473

Security Classification

2

PAPER NO. 13

ON SOME GEOMETRIC PROPERTIES OF HUMAN RIBS-I

Sanford B. Roberts and Ping Heng Chen

School of Engineering and Applied Science
University of California, Los Angeles

ABSTRACT

The cross-sectional geometric properties of ribs 1 through 8 of a medium-framed female cadaver specimen were studied. Specifically, each rib was cut into 10 sections, the exposed cross-sections photographed, a finite element grid superimposed, and with the aid of a digital computer, the geometric properties (total area, compact bone area, centroid, principal axes, principal moments of inertia and torsional constant) of the compact bone region were determined. Although most of these quantities exhibit wide variations some trends do emerge. Of particular significance is a simple geometric construction for the location of the centroid and principal axes and the general result that a thin-walled ellipse is a reasonably accurate model from which the approximate cross-sectional properties may be calculated.

INTRODUCTION

Human ribs can be categorized as "long bones," (Frost 1967)* in that they possess the characteristic structure of a thin cortex of compact bone surrounding a medullary canal of marrow and trabecula. The architecture of long bones (especially the femur) and its relationship to the load carrying function has been studied since the later part of the 19th century (Evans 1957). There have also been attempts at detailed stress analysis with the usual objective of relating the shape of the compacta and trabecula to a simplified notion of the stress and/or strain state under load (Evans 1957). In spite of an extensive history (Evans 1967) of investigations, there do not appear in the literature any significant studies which provide detailed quantitative data on the geometry, especially cross-sectional geometry, of any human bones. It goes without saying that a meaningful stress analysis (e.g. Roberts 1970) of the components of the skeletal system under normal or traumatic conditions is impossible without knowledge of (among other things) the geometry. As part of a study of the response of the

*See list of References at end of paper.

thoracic skeleton to dynamic forces, a program aimed at defining the cross-sectional and global properties of human ribs was undertaken. This is a first report, focusing upon our findings within the cross-sections of human ribs.

The judgment was made at the outset that the trabecula would be neglected and only the compact bone geometry would be considered. Since the geometric quantities determined are those necessary for stress analysis, this decision implies that the compact bone is the primary load carrying component whereas the contribution of the cancellous bone is insignificant. Although it appears intuitively correct, this hypothesis requires further experimental evidence for its full justification.

The information presented herein was obtained by direct observation and measurements on the rib cage of an embalmed female cadaver specimen with an apparent small frame. The cause of death was coronary vascular arteriosclerosis in June 1968 at age 77.

Observations made on one cadaver specimen are hardly sufficient to permit drawing general conclusions. We are however, strongly motivated to find conceptually simple unifying principles from which approximate geometric properties of typical ribs can be constructed. For example, it would be advantageous to be able to make two measurements (say "width" and "depth") at a particular station along the longitudinal axis of a rib and calculate the cross-sectional properties, such as location of centroid and principal moments of inertia, without actually exposing the internal cross-section and making direct measurements. Motivated by this objective we have intentionally flavored this report with what appear to be generalizations applicable to most human ribs. We trust that a desire on the part of other researchers to further substantiate or contradict our hypotheses will help stimulate the production of a statistically valid collection of data.

EXPERIMENTAL AND ANALYTIC PROCEDURES

The rib cage from the specimen 6901 was excised, the individual ribs (designated 6901-Rib Number) separated and the superficial soft tissue was removed. Each rib (except No. 1) was cut into 10 sections (see Fig. 1), the cuts being made in a plane approximately normal to the longitudinal axis of the rib. The longitudinal axis being approximated by the imaginary line parallel to the superior and inferior borders and halfway between them. The interior surface thus exposed is designated herein as the rib cross-section. The cross-section contains two regions, namely a thin border of compact bone and an interior region of cancellous bone and marrow. From the perspective that the bony thorax is a force transmitting structure, only the compact bone is considered effective. Consequently, it is to it which our attention is directed. The compact bone region is not easily distinguishable from the cancelleous bone interior. The interior "border" requires careful scrutiny and judgement for its definition. We found that close examination under magnification, and the removal of all soft tissue and

as much cancellous bone as possible is necessary since it would otherwise render the border definition extremely difficult.

The exposed cross-sections of each rib were photographed under 10 power magnification with a scale having 0.01 in. divisions placed in the field of view and in the plane of the cross-section (Figs. 2-6) Tracings of the outline of the compact bone regions were made from the developed photographs. A network of 36 quadrilateral elements (72 nodal points) and a cartesian coordinate system describing the geometry of the cross-section* was then superimposed. The coordinates of each nodal point were scaled and entered as input data into an augmented finite element computer program (Mason 1967) which calculated

a) The cross-sectional area of compact bone (A_c) and total cross-sectional area (A_t)

b) The orientation of the principal axes (y,z) of inertia

c) The location of the centroid

d) The principal moments of inertia

$$I_y = \int_R y^2 dA, \quad I_z = \int_R z^2 dA \qquad R = \text{Compact bone region}$$

e) The torsional constant (J), where

$$J = \int_R \left[y^2 + z^2 + y \frac{\partial \phi}{\partial z} - z \frac{\partial \phi}{\partial y} \right] dA \tag{1}$$

$$\frac{\partial^2 \phi}{\partial y^2} + \frac{\partial^2 \phi}{\partial z^2} = 0 \tag{2}$$

where $\phi = \phi(y,z)$ = St. Venant warping function

The calculation of the torsional constant (J) based upon Equations (1) and (2) and appropriate boundary conditions assumes, among other things, that the material is isotropic in that $G_{xz} = G_{yx}$ (G = elastic shear modulus). Although there is strong evidence (Dempster 1952) indicating that bone is not isotropic, there is presently insufficient information on the dependence of the shear modulus upon orientation normal to the long axis of the bone. This is, at this time it is reasonable to assume that $G_{xz} = G_{yx}$.

In addition to the "exact" analysis described above, an approximate analysis based upon

a) The assumption that the cross-section is a thin-walled ellipse with constant effective thickness (t_e)

*Hereinafter the term cross-section will refer to the compact bone portion thereof unless otherwise defined.

b) The use of the actual "major" and "minor" axes (A,B) measured along actual principal axes, and the ratio of compact bone to total cross-sectional area A_c/A_t

was carried out.

In a thin-walled elliptic cross-section, using a) above it can be readily shown that (see Hudson 1917 and Shanley 1957)

$$4\,t_e = (A+B) - \sqrt{(A+B)^2 - 4\beta AB} \quad , \quad \beta = \frac{A_c}{A_t} \tag{3}$$

$$64I_y = \pi\,[BA^3 - (B-2t_e)\,(A-2t_e)^3]$$
$$64I_z = \pi\,[B^3A - (B-2t_e)^3(A-2t_e)] \tag{4}$$

$$J = \frac{4\,a^2 t_e}{s}$$
$$a = \frac{\pi(A-t_e)(B-t_e)}{4}$$
$$s = \frac{\pi(A+B)}{8}\left[3(1+\lambda) + \frac{1}{1-\lambda}\right] \tag{5}$$
$$\lambda = \left[\frac{A-B}{2(A+B)}\right]^2$$

GENERAL RESULTS

The shape of the thin wall of compact bone in the typical rib cross-section is more or less "elliptic." It can be qualitatively characterized by the ratio of the lengths along the "minor" and "major" principal axes (B/A). Figure 7 shows a plot of B/A as a function the nondimensional position parameter (S/L) for ribs 6901-3 thru 6901-8. Observe that at the costochondral junction (S/L=0) the compact bone shape is somewhat cylindrical ($0.5 \leq B/A \leq 0.8$). Proceeding posteriorly into the shaft region it immediately begins to flatten ($0.2 \leq B/A \leq 0.4$) and then gradually expands becoming more "cylindrical" again approaching the angle with maximum values of B/A in the neighborhood of the tubercle.

THICKNESS OF COMPACT BONE

The thickness (t) of the compact bone cortex varies both as a function of S/L and within each cross-section without any apparent pattern in either respect. The maximum and minimum values of t where measured in each cross-section and plotted as a function of S/L. These curves for ribs 3, 5 and 7 are shown in Figs. 8 to 10. The value of t_{min} is reasonably constant over the rib length, being on the order of 0.01 in. for the three ribs. However, t_{max} exhibits extensive excursions along the length of any one particular rib. The peak values are usually associated with a highly localized thickened region in a cross-section.

The equivalent thickness (t_e) given by Equation (3) was also plotted in Figs. 8 to 10. It is interesting to note that t_e is reasonably close to the median wall thickness.

PRINCIPAL AXES OF INERTIA AND CENTROID

The calculated location of the centroid (c.g.)* and the orientation of the principal axes of inertia for specimen 6901-3 Sections 1, 3, 5, 7 and 9 are shown in Figs. 2 to 6. Note that the compact bone boundary has been exagerated and the principal axes superimposed upon the actual photographs of the cross-sections. One observes that the centroid is approximately at the center of the overall cross-section and that the minor principal axis is nearly parallel to a line connecting the extremum points. The observation suggests the following construction procedure for the approximate centroid location and the local orientation of the principal axes (refer to Fig. 11).

a) Connect the two points (a_1 and a_2) on the extreme superior and inferior edges by a straight line.

b) Enscribe the outer boundary with a rectangle having sides parallel and perpendicular to $a_1 - a_2$.

c) The intersection of the diagonals of this rectangle locates the c.g. and lines through the c.g. parallel and perpendicular to $a_1 - a_2$, are the minor and major principal axes respectively.

The accuracy of this procedure was tested using ribs, 6901-3, 5 and 7. The actual c.g. was located and its position compared with that of the approximate c.g. (designated c.g'.) by the dimensions δ_A and δ_B (Fig. 11). Also, the angular orientation, α of the approximate principal axes (y' and z'), with respect to the actual principal axes (y,z) was determined. The relative magnitudes of these quantities are given in Table 1. We observe that

*Under the assumption that rib compact bone is homogeneous we will use the designations centroid and center of gravity (c.g.) interchangeably.

TABLE 1

RIB NO.- SEC.	S/L	δ_A (in)	A (in)	δ_A/A %	δ_B (in)	B (in)	δ_B/B %	α Deg.
3-1	0.0	0.010	0.485	2.06	0.005	0.305	1.64	7.0
3-2	0.104	0.005	0.550	0.90	0.002	0.135	1.48	0.5
3-3	0.200	0.002	0.550	0.36	0.002	0.130	1.54	2.0
3-4	0.306	0.011	0.510	2.16	0.001	0.125	0.80	2.0
3-5	0.392	0.010	0.485	2.06	0.010	0.175	5.70	1.0
3-6	0.485	0.010	0.440	2.27	0.023	0.210	10.90	2.0
3-7	0.598	0.020	0.360	5.55	0.004	0.210	1.90	7.2
3-8	0.695	0.012	0.375	3.20	0.030	0.200	15.00	5.5
5-1	0.0	0.030	0.545	5.50	0.038	0.342	11.10	10.0
5-2	0.125	0.010	0.580	1.73	0.00	0.165	0.00	0.0
5-3	0.241	0.010	0.498	2.01	0.00	0.175	0.00	1.2
5-4	0.345	0.035	0.410	8.54	0.005	0.192	2.60	1.75
5-5	0.427	0.030	0.378	7.94	0.00	0.240	0.00	1.0
5-6	0.618	0.012	0.430	2.79	0.012	0.235	5.10	3.3
5-7	0.740	0.032	0.370	8.65	0.026	0.280	9.30	3.3
7-1	0.0	0.046	0.570	8.10	0.020	0.280	7.14	2.5
7-2	0.107	0.008	0.610	1.30	0.010	0.210	4.76	5.5
7-3	0.238	0.028	0.530	5.30	0.020	0.200	10.00	4.0
7-4	0.352	0.001	0.527	1.90	0.017	0.200	8.50	2.0
7-5	0.527	0.030	0.505	5.95	0.007	0.240	2.92	4.5
7-6	0.665	0.060	0.520	11.50	0.025	0.264	9.47	1.5
7-7	0.775	0.005	0.475	1.05	0.028	0.300	9.35	6.0

$$\frac{\delta_A}{A} < 12\%, \quad \frac{\delta_B}{B} < 15\%, \quad |\alpha| < 10^\circ$$

with the average values for the three ribs being

$$\left.\frac{\delta_A}{A}\right|_{avg.} \simeq 4\%, \quad \left.\frac{\delta_B}{B}\right|_{avg.} \simeq 5\%, \quad |\alpha|_{avg} \simeq 3.5^\circ$$

Considering the inherent inaccuracies in defining the compact bone boundaries, these errors are within acceptable limits.

CROSS-SECTIONAL AREA

The cross-sectional area of compact bone A_c (see Figs. 12 to 15) is reasonably constant over the entire length of each rib (especially in the shaft) showing significant perturbations only in the tubercle-neck region and in some cases at the costochondral junction. The value of A_c at the costochondral junction (CC.J.) is particularly difficult to determine due to the indistinct transitioning of cartilage to bone. In particular, ribs 5 and 6 showed extensive ossification at this location, thereby giving rise to relatively large values of A_c. In the shaft region of a typical rib A_c is of the order 0.035 in.^{2}

The calculated values of A_c, based upon an elliptic cross-section shape produces an excellent approximation. This appears to be uniformly true except at a few isolated sections wherein there is a sharply indented costal groove.

The ratio of A_c to the area of the entire cross-section (A_t) for ribs 1-8 is shown in Fig. 16. The average values of A_c/A_t are greatest for ribs 1 and 2, (approximately 60% and 50% respectively) decreasing with increasing rib number to essentially a constant 40% in the shaft region of ribs 5-8. The values at the costochondral junction of ribs 5-8 are quite erratic primarily due to the poor definition of this junction as an apparent consequence of cartilage ossification.

MOMENTS OF INERTIA AND TORSIONAL CONSTANT

The calculated principal moments of inertia (I_y, I_z) and the torsional constant J are given in Figs. 12 to 15. These quantities are "second moments" of area and are therefore more sensitive to shape and thickness variations than is A_c. This is exemplified by the lack of uniformity over the length and the more violent changes. For ribs 3-6 the largest values occur at the costochondral junction where the cross section is "flared-out" ($B/A > 0.5$), whereas for ribs 7 and 8, maximum values occur in the tubercle region. Typical values in the shaft region (e.g. for rib 7) are

$$I_y = 0.0007 \text{ in.}^4, \quad I_z = 0.0002 \text{ in.}^4, \quad J = 0.0005 \text{ in.}^4$$

Surprisingly, the results from the elliptic approximation compare favorably with the actual values. There are, of course, isolated regions wherein marked irregularities such as deep costal grooves (e.g. rib 7 Section 6) produce poor agreement.

CONCLUSIONS

An analysis of the cross-sectional properties of the first 8 ribs from a female cadaver has been conducted. We have found that the quantities studied (t, A_c, A_c/A_t, I_x, I_y, J) show considerable variation as a function of position along each rib as well as variation between ribs. However, it is also clear that at least for this specimen, certain definite patterns do emerge.

a) The median wall thickness is greatest in the vicinity of the tubercle.

b) The compact bone region, c.g. and principal axes of inertia can be approximately located by a simple geometric construction.

c) The compact bone ratio (A_c/A_t) is greatest in rib 1 decreasing to a relatively constant value of about 40% in the shaft regions of ribs 5-8.

d) All of the geometric quantities studied possess a characteristic variation with rib number. That is, a decrease from rib 1 to a local minimum at rib 3 followed by an increase to a local maximum at ribs 6 or 7 and decreasing thereafter.

e) The geometric properties can be calculated with reasonably good accuracy by assuming the rib cross-section to be a thin-walled ellipse, provided the major and minor axes and the compact bone ratios are known.

In order to obtain upper-bound estimates of the cross-sectional properties of human ribs, an analysis similar to that described herein has been initiated on a large-framed male specimen. Preliminary results indicate that values of the various geometric quantities in the shaft regions are approximately 20% higher than those of specimen 6901.

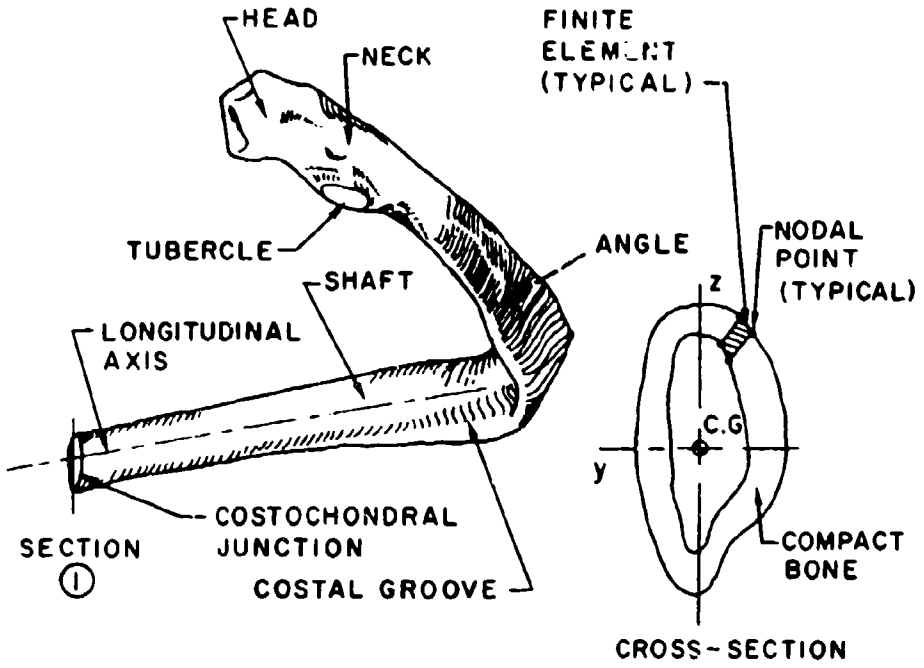

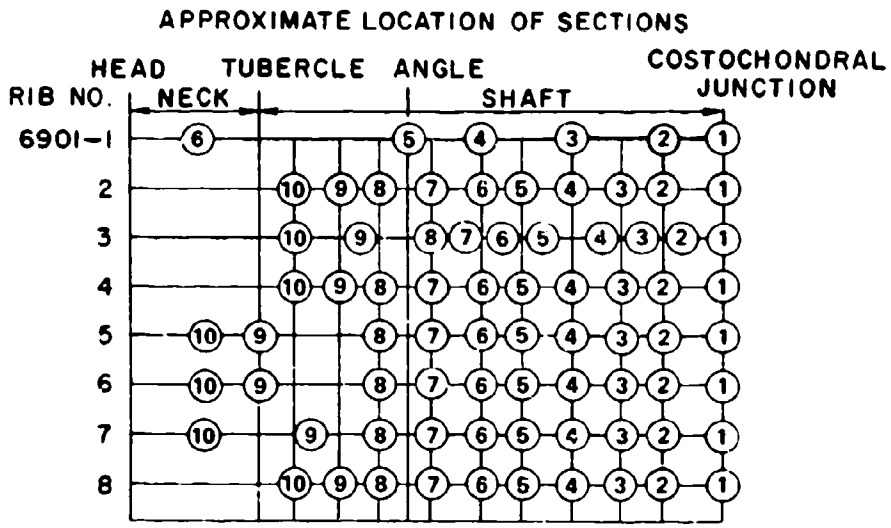

Figure 1. Rib nomenclature and approximate location of cross-sections

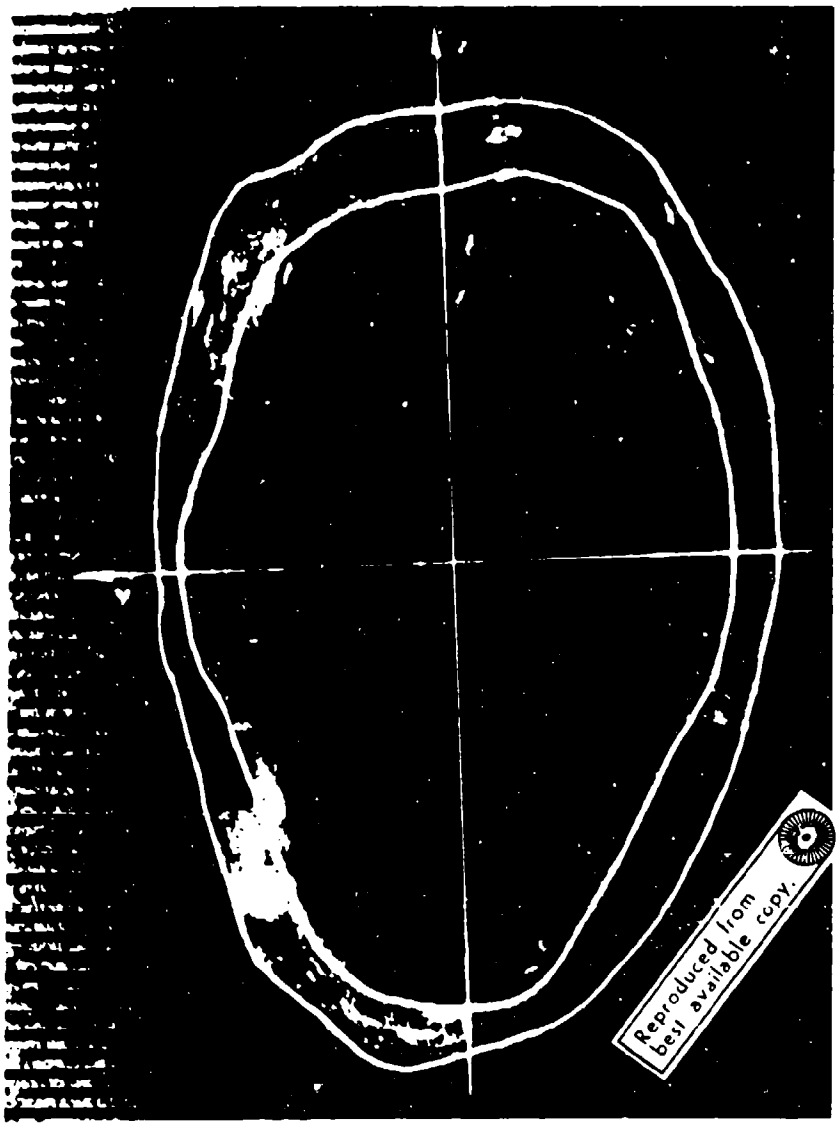

Section 1
S/L=0.0

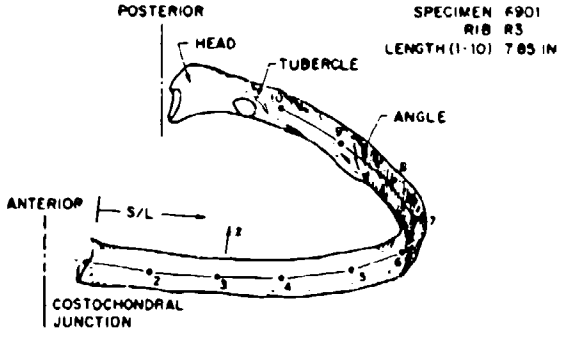

Figure 2. Rib 6901-3 Section 1

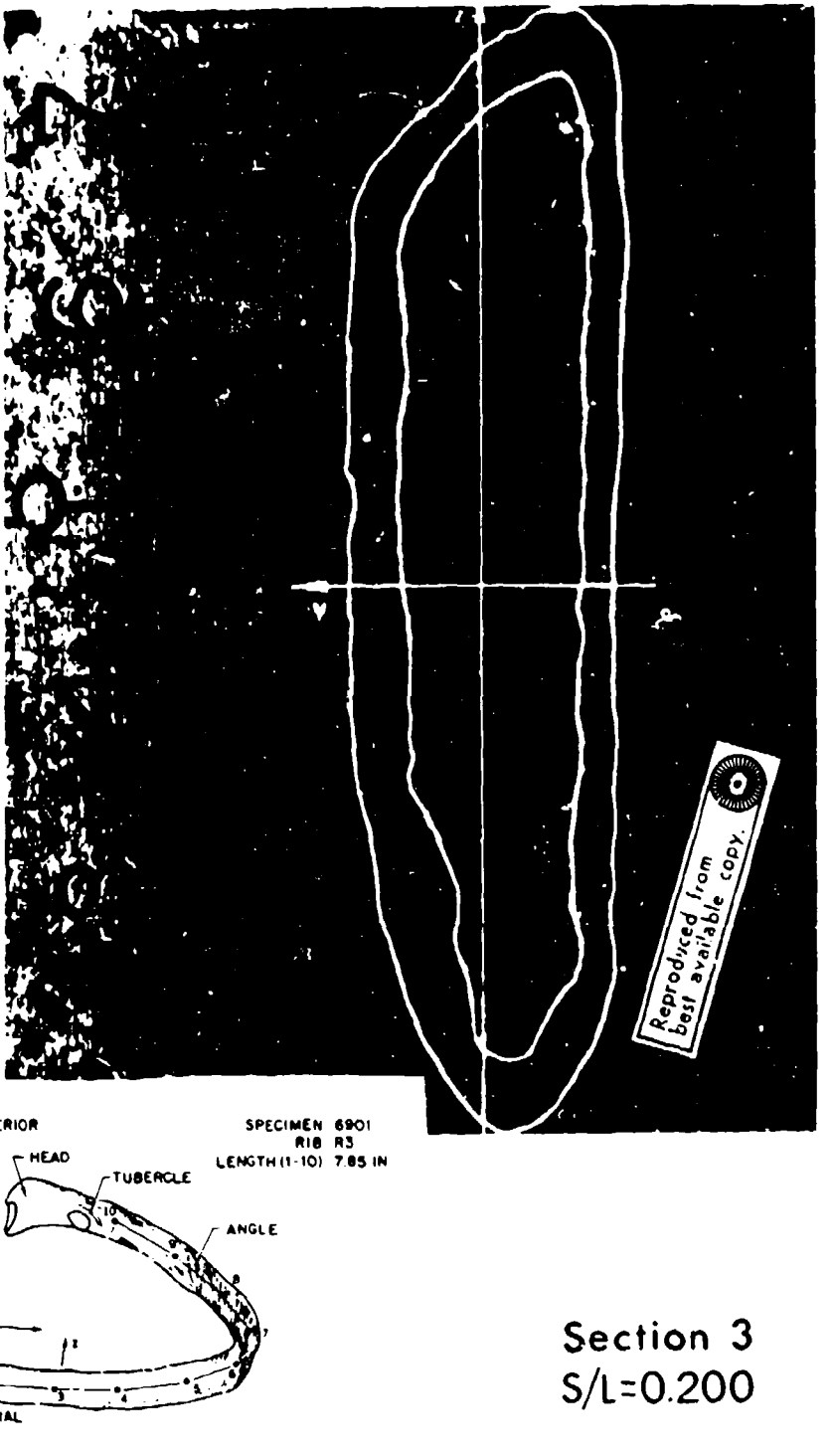

Figure 3. Rib 6901-3 Section 3

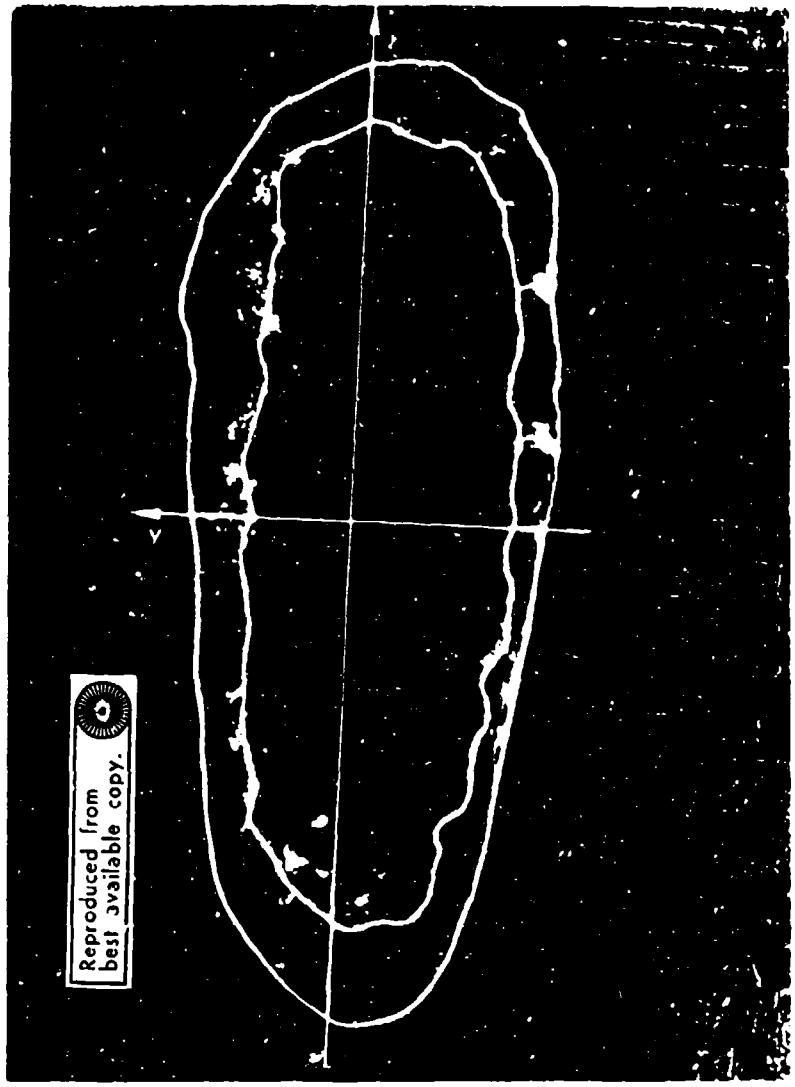

Section 5
S/L=0.392

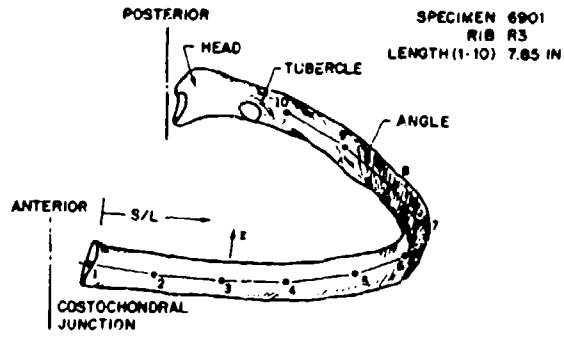

Figure 4. Rib 6901-3 Section 5

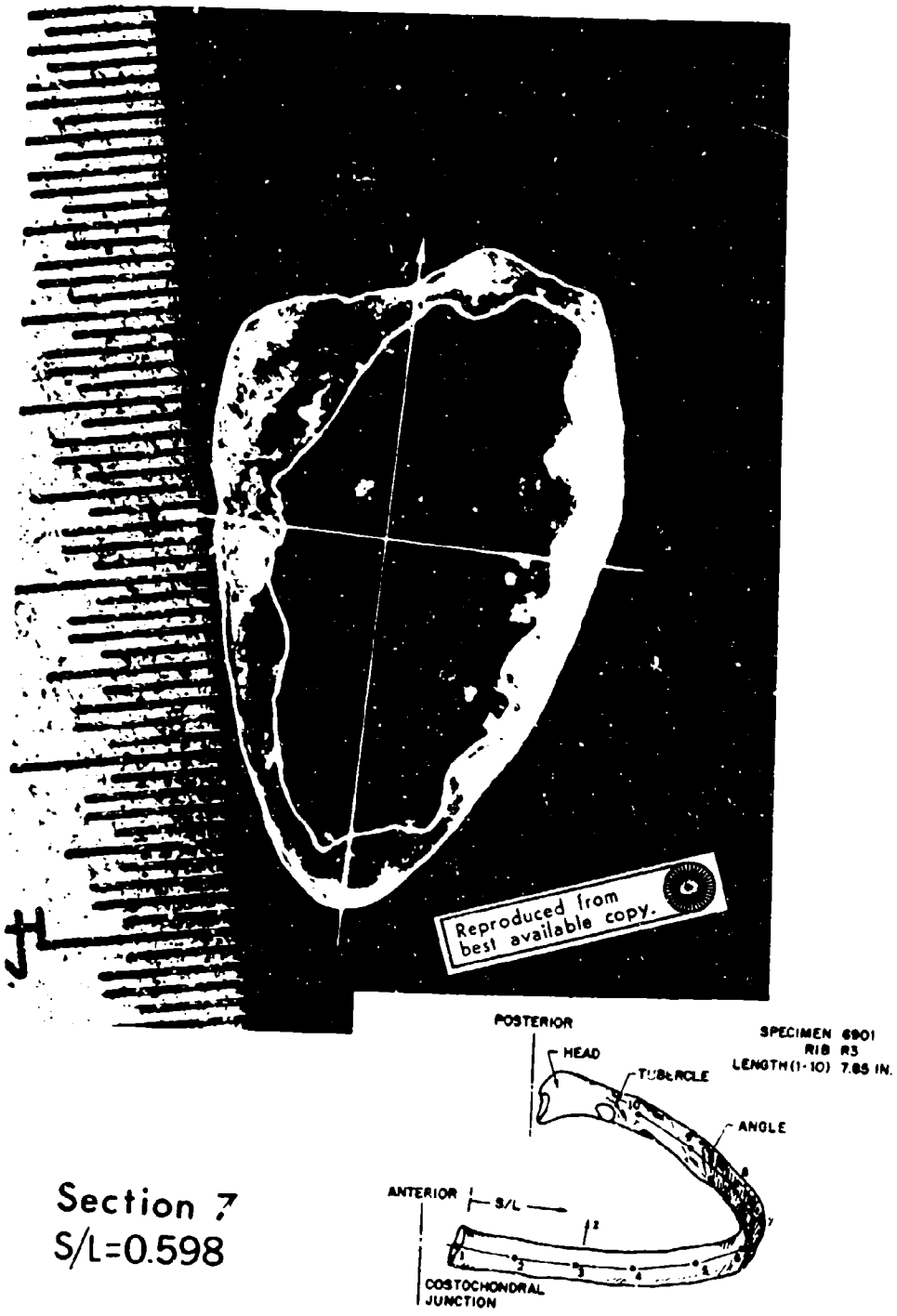

Figure 5. Rib 6901-3 Section 7

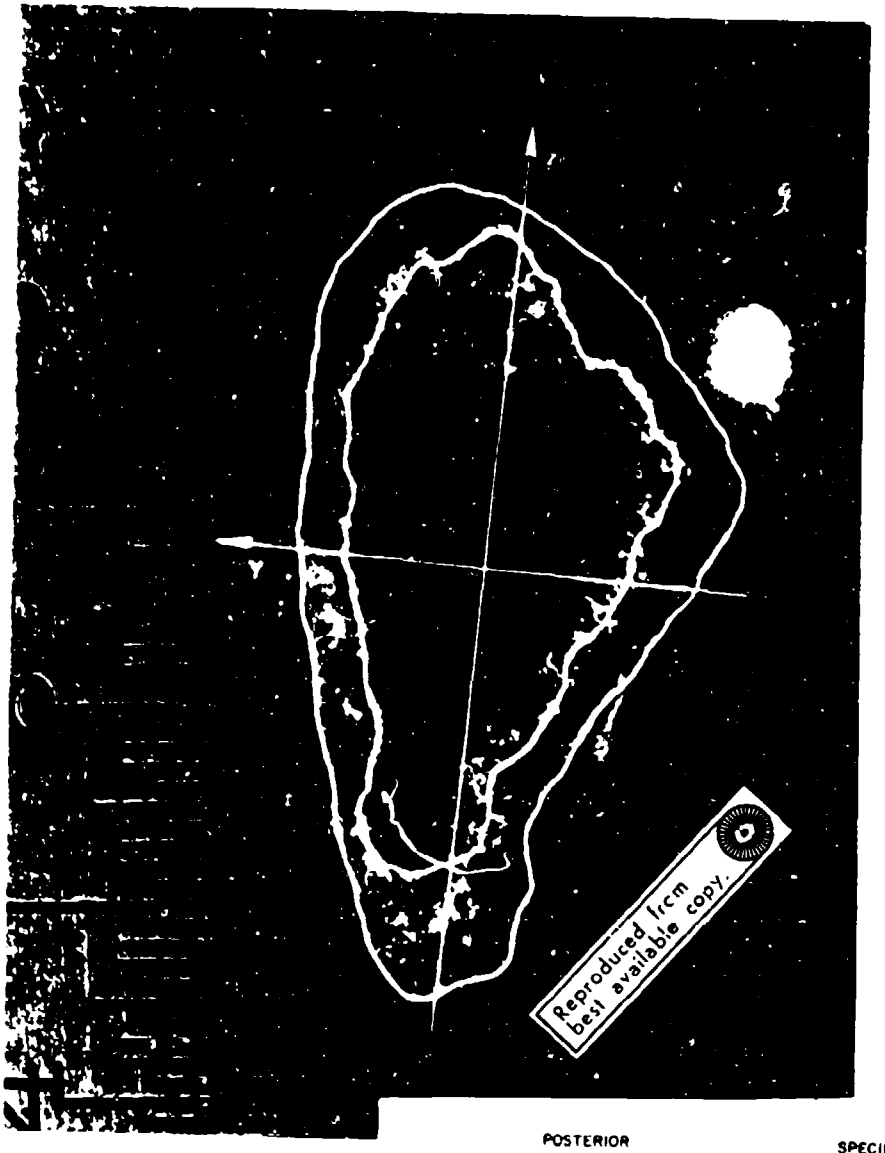

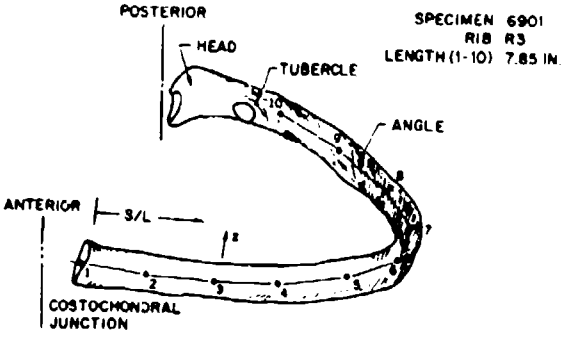

Section 9
S/L=0.801

Figure 6. Rib 6901-3 Section 9

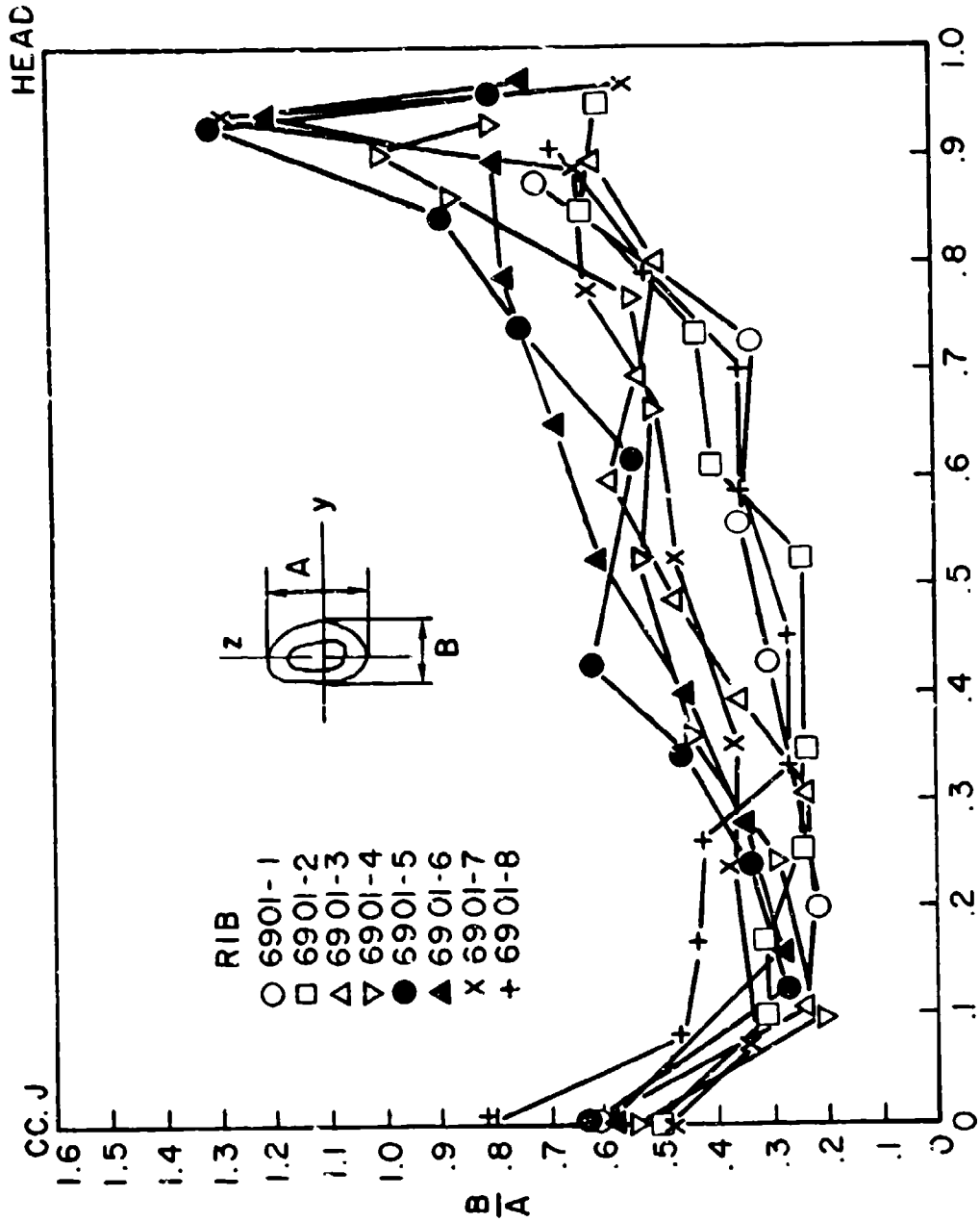

Figure 7. Ratio of principal dimensions (B/A) vs. S/L

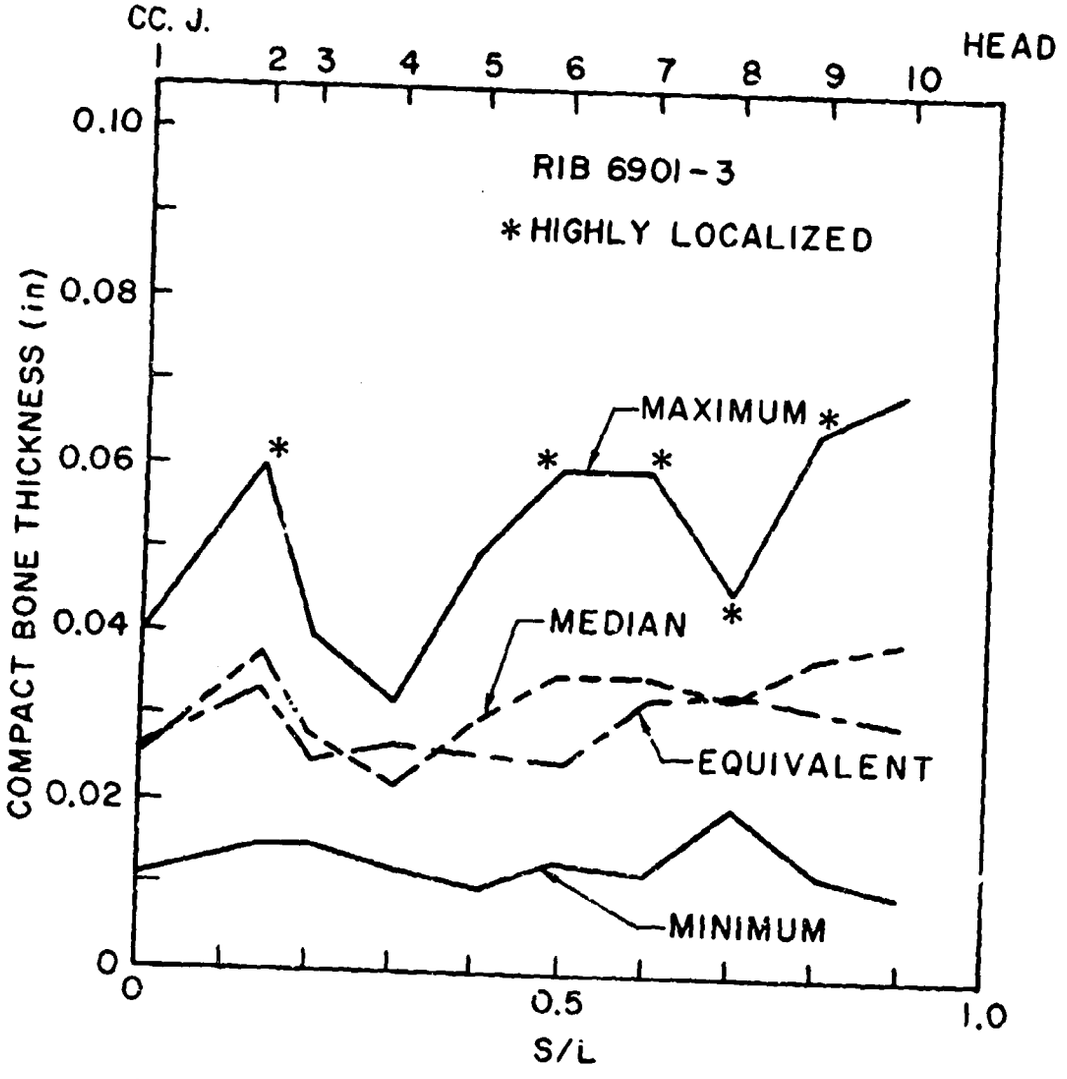

Figure 8. Rib 6901-3 Compact bone thickness vs. S/L

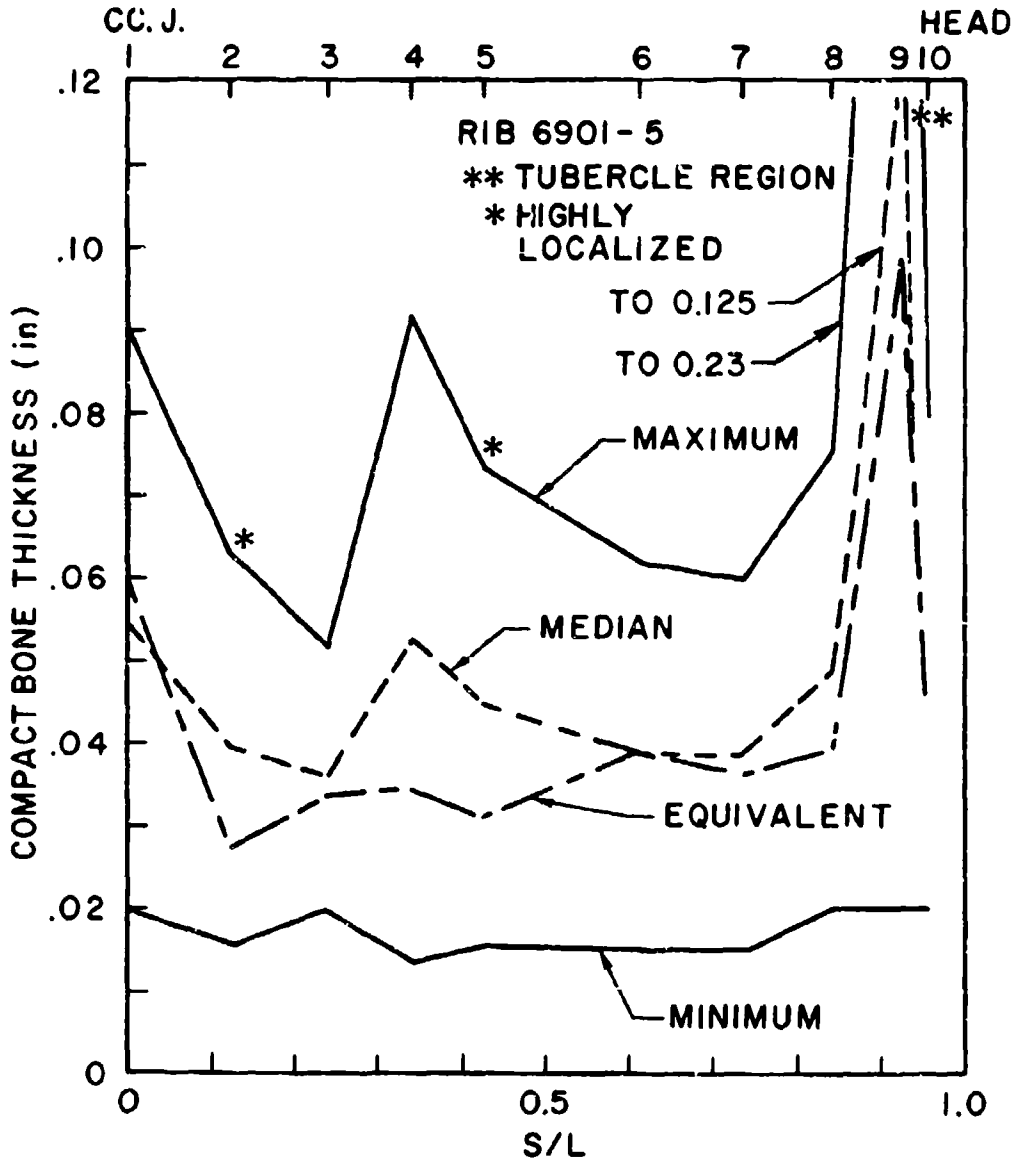

Figure 9. Rib 6901-5 Compact bone thickness vs. S/L

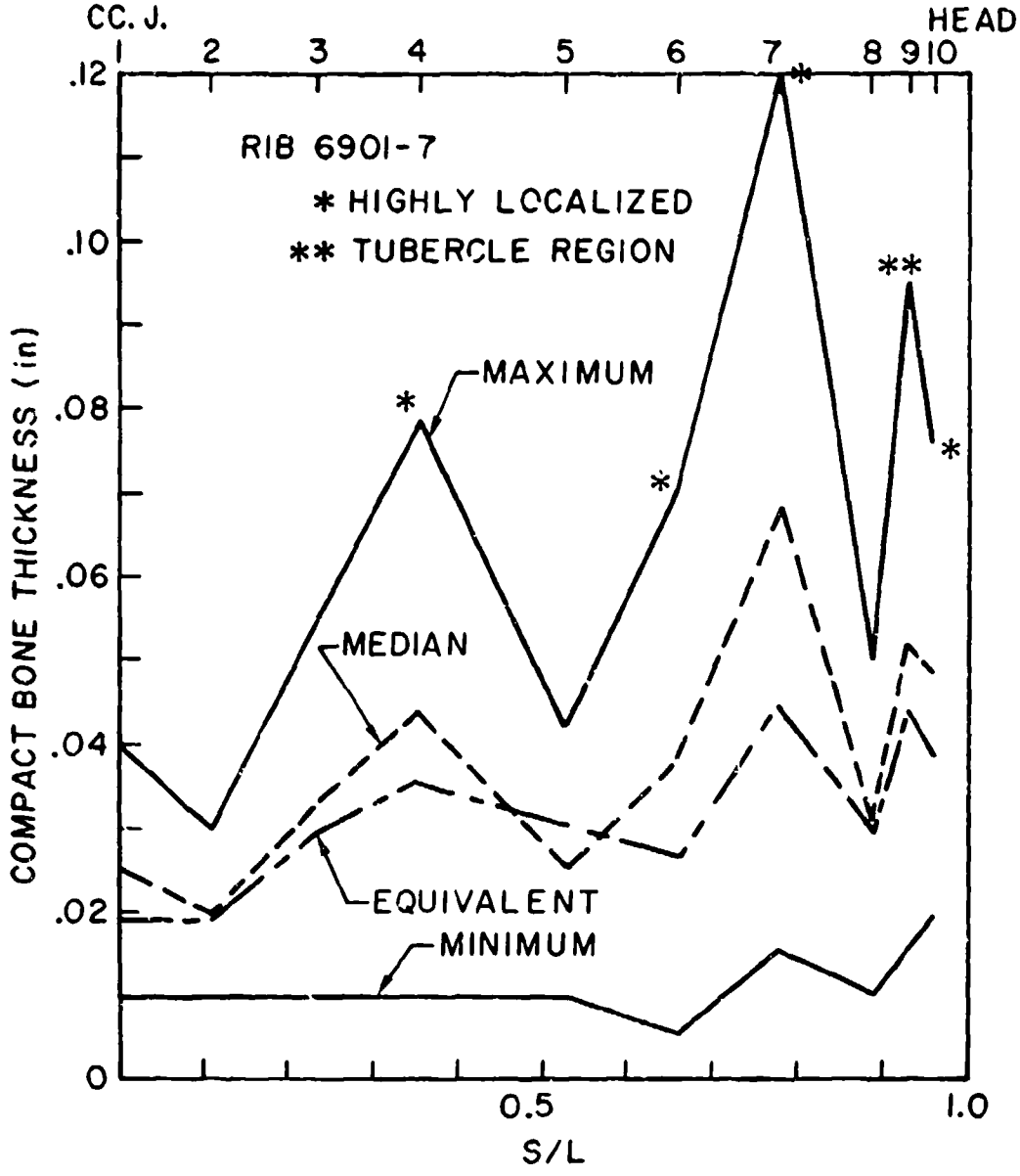

Figure 10. Rib 6901-7 Compact bone thickness vs. S/L

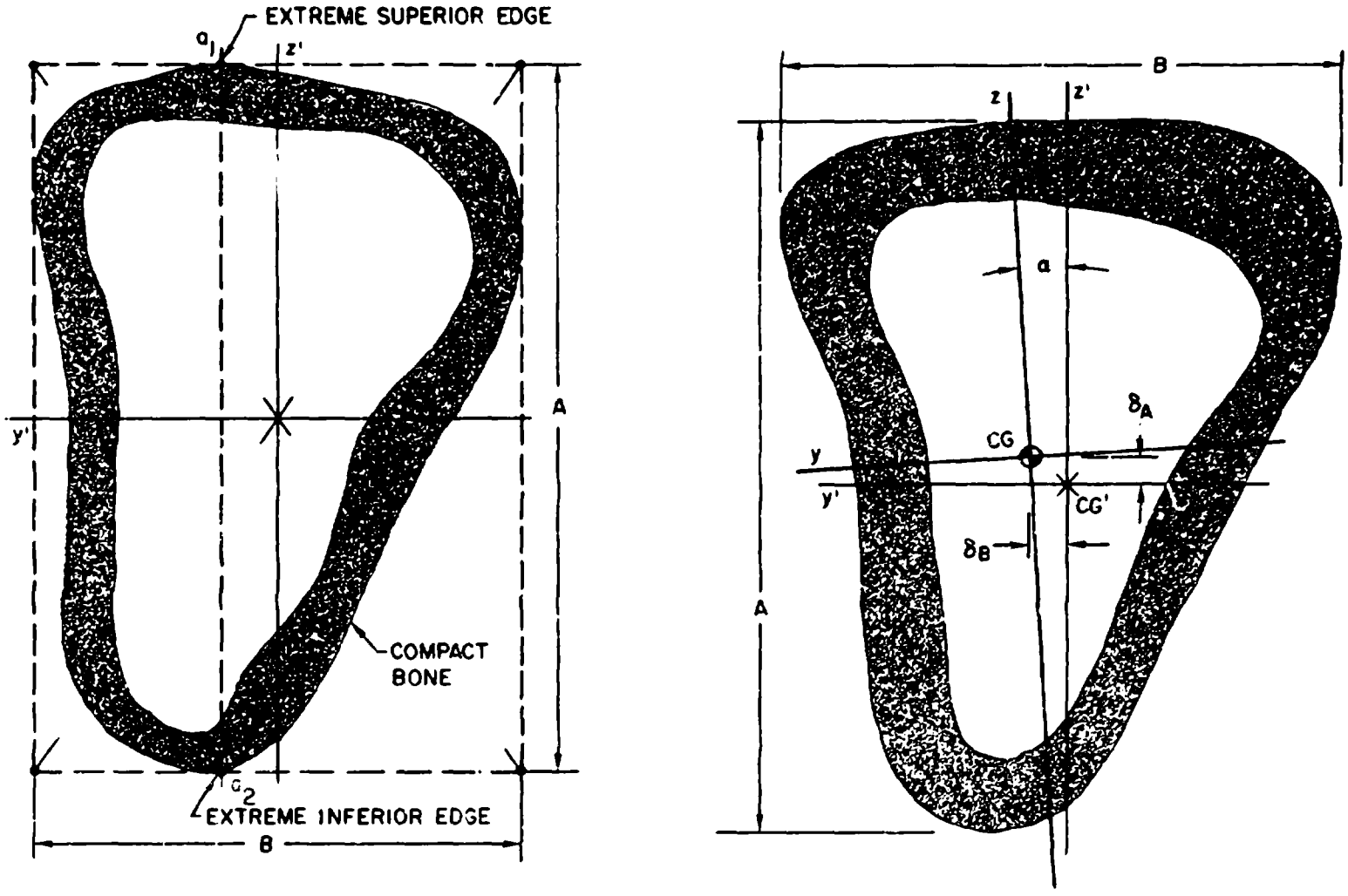

Figure 11. Construction of centroid and principal axes

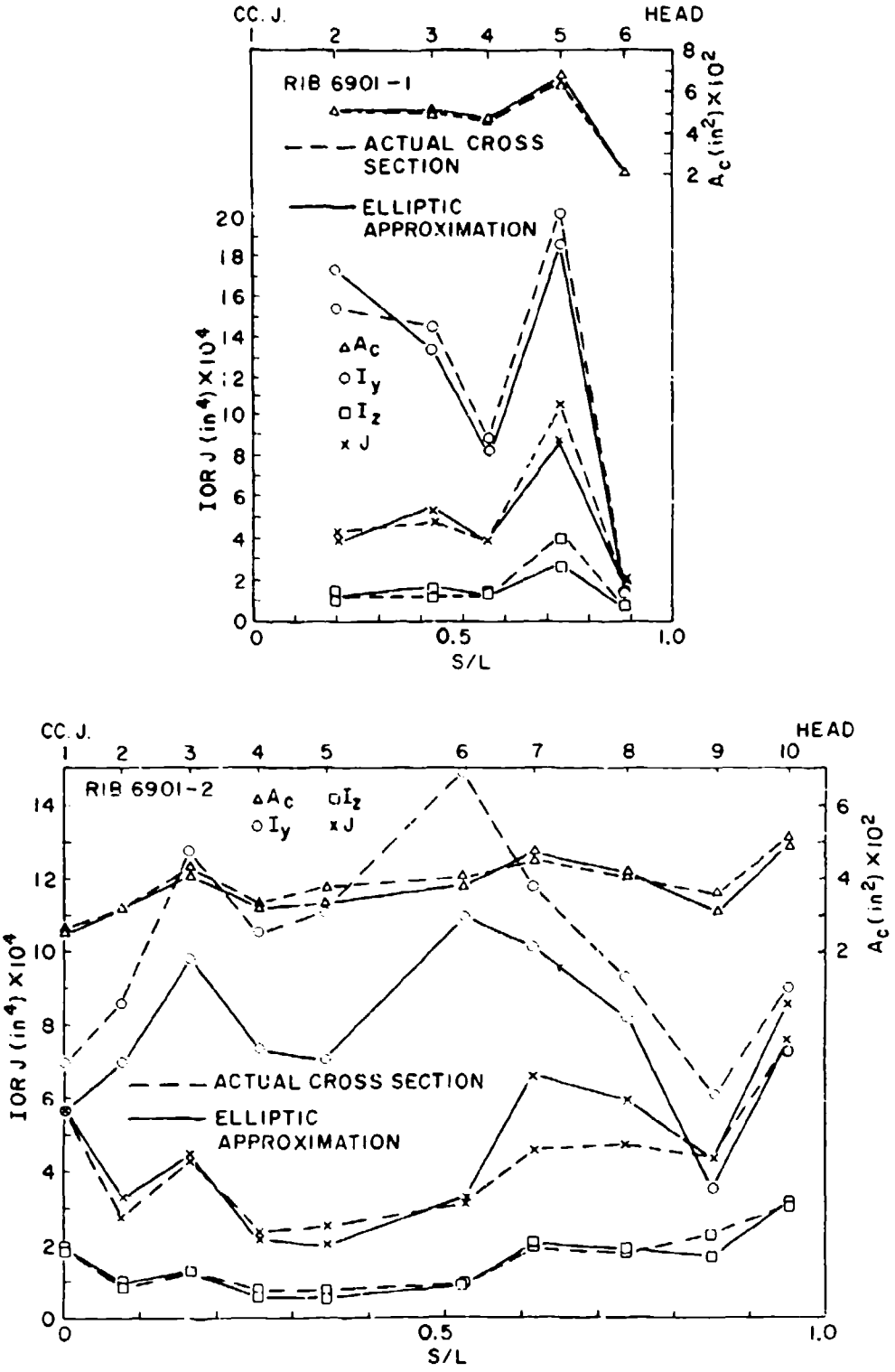

Figure 12. Cross-sectional properties of ribs 6901-1, 6901-2 vs. S/L

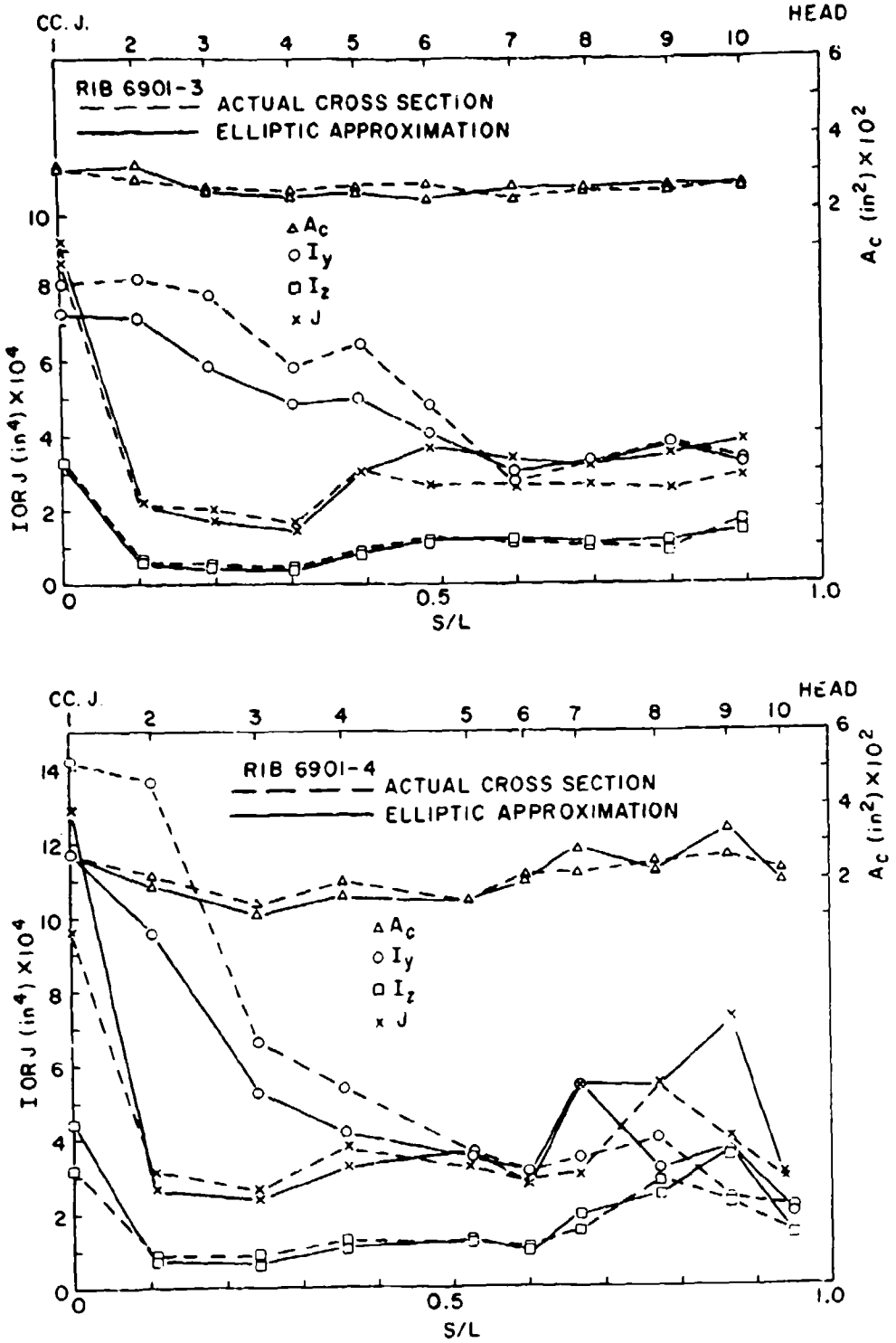

Figure 13. Cross-sectional properties of ribs 6901-3, 6901-4 vs. S/L

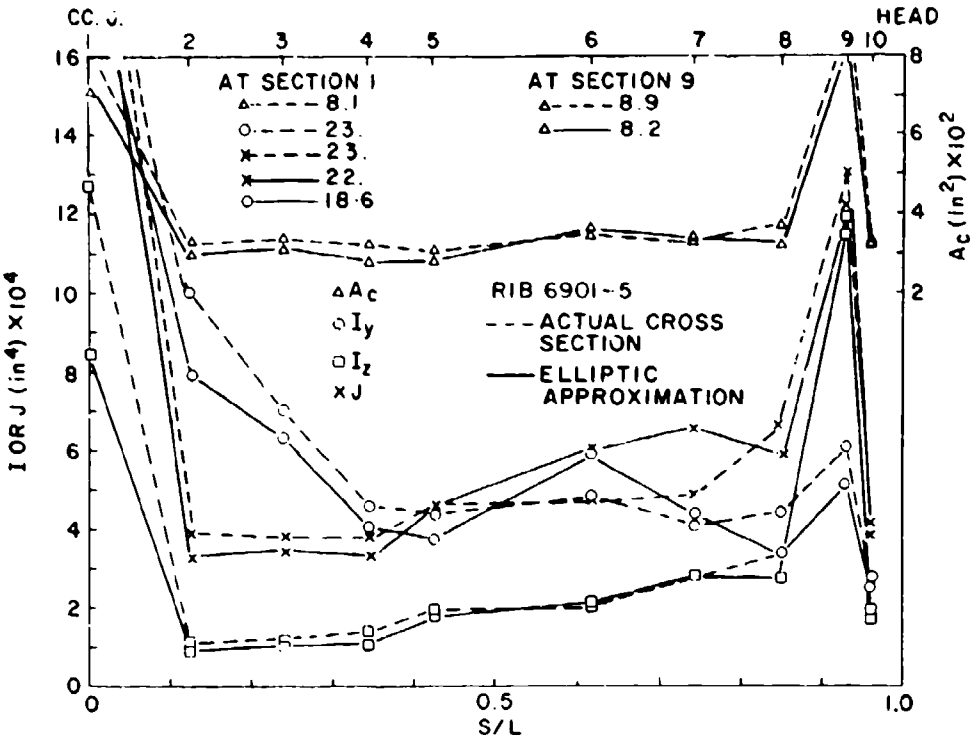

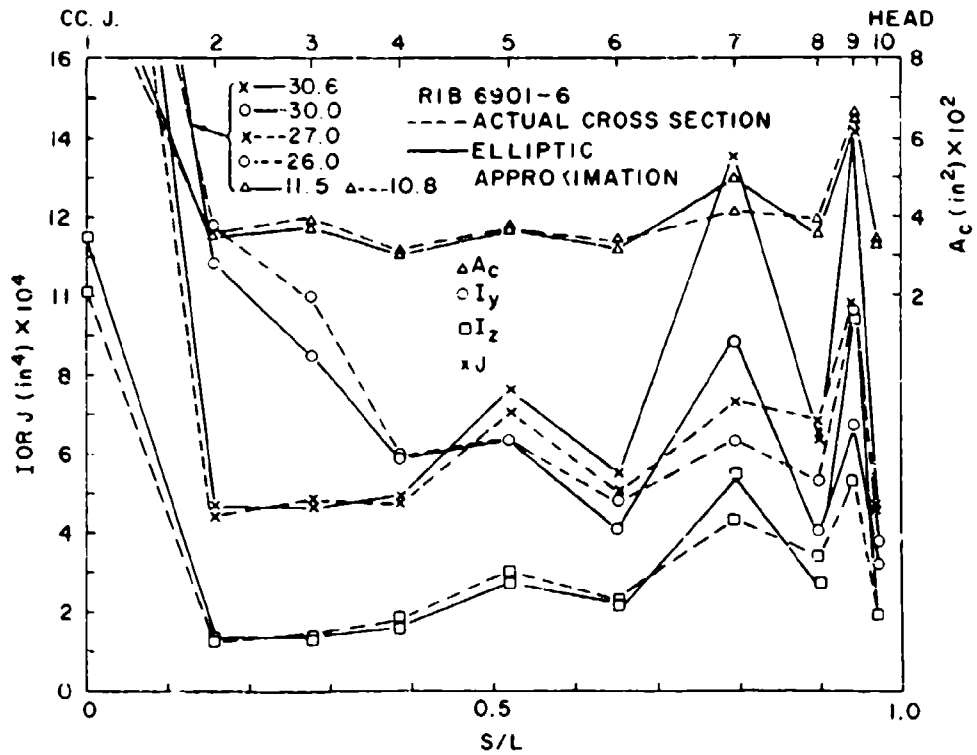

Figure 14. Cross-sectional properties of ribs 6901-5, 6901-6 vs. S/L

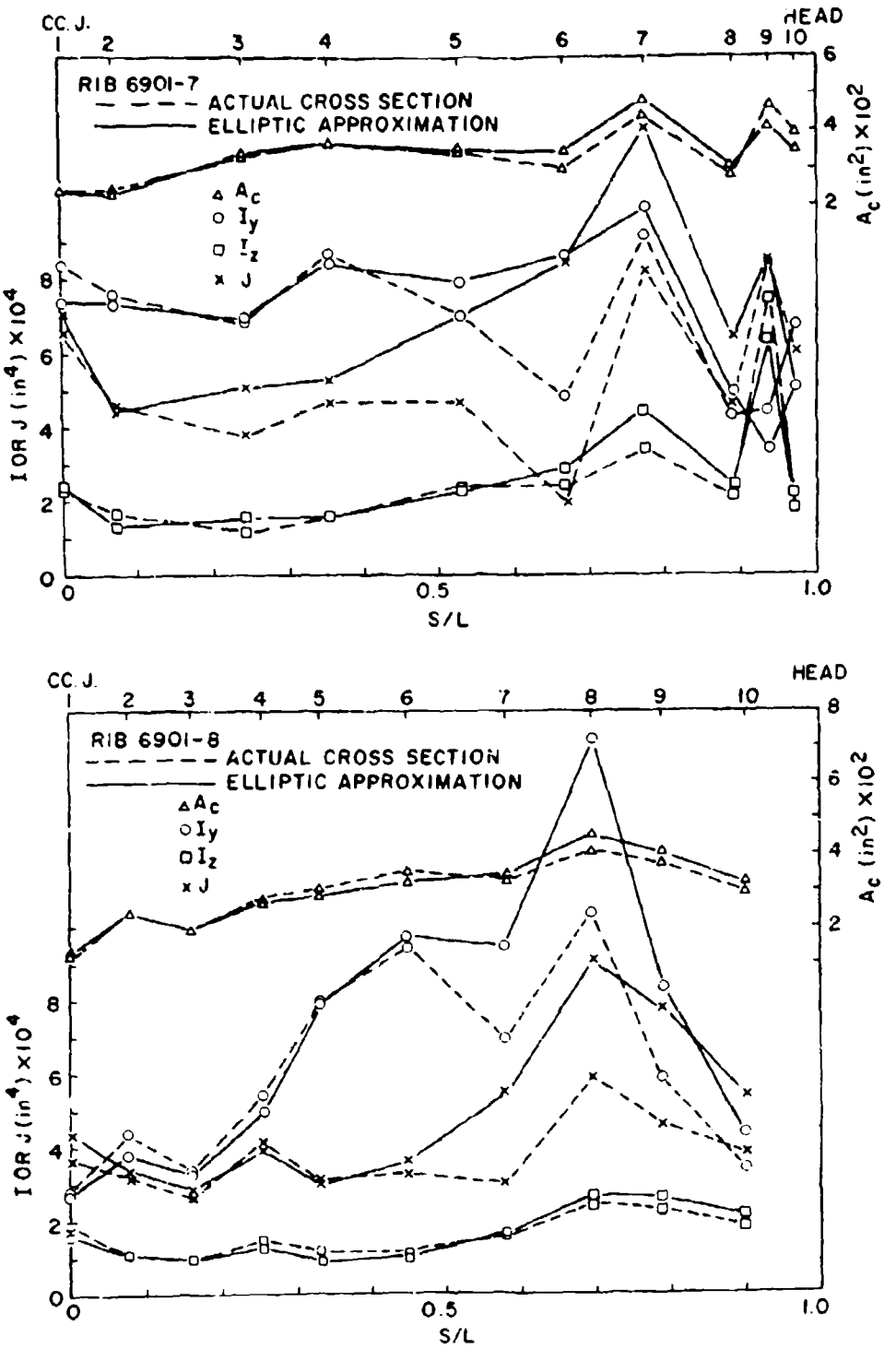

Figure 15. Cross-sectional properties of ribs 6901-7, 6901-8 vs. S/L

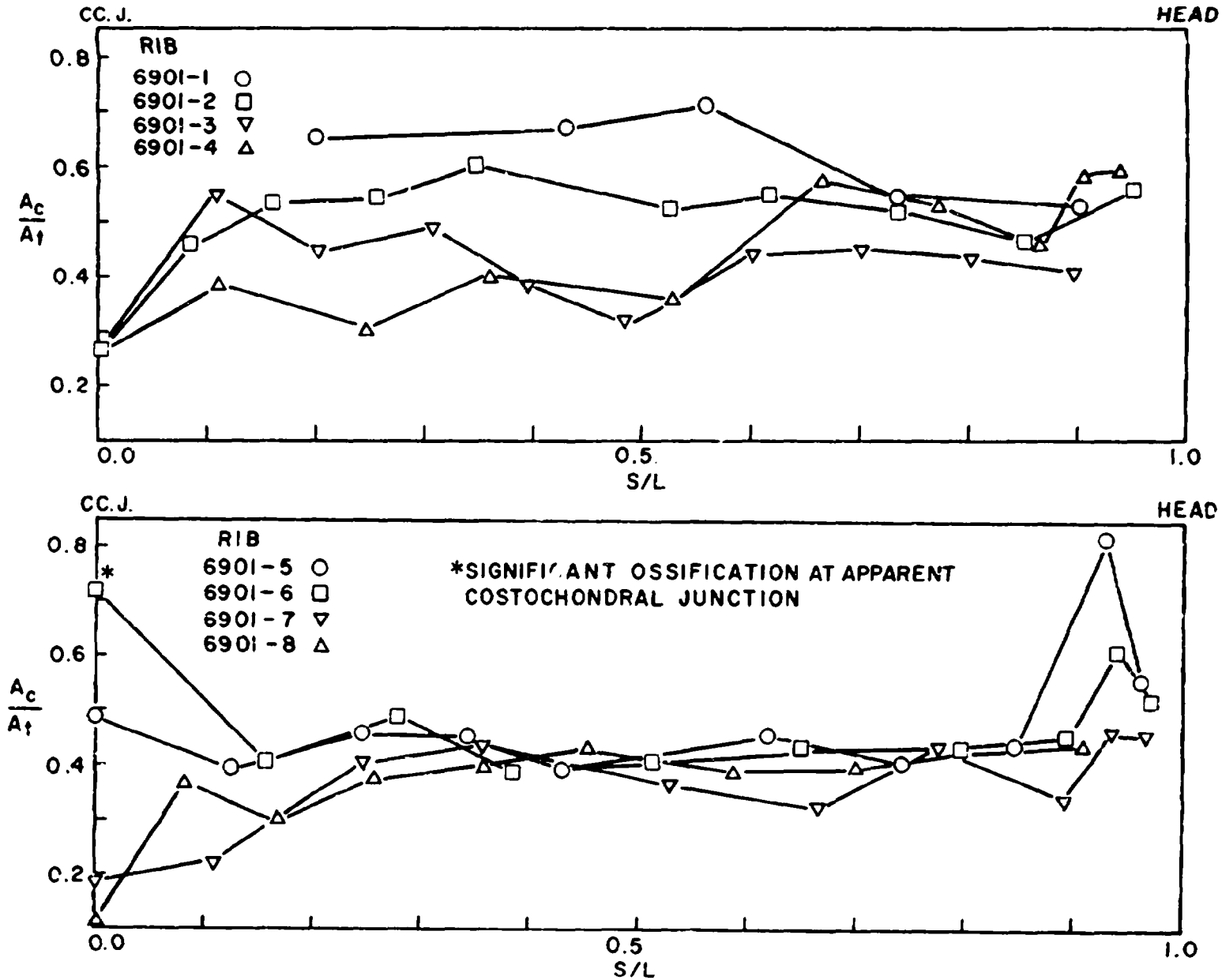

Figure 16. A_c/A_t vs. S/L for ribs 6901-1 through 6901-8

REFERENCES

26

1. Dempster, W.T., Liddicoat, R.T., (1952) Compact Bone as a Non-Isotropic Material, The American Journal of Anatomy, Vol. 91, No. 3.

2. Evans, F.G., (1957) Stress and Strain in Bones. Ed. O. Glasser, Charles C. Thomas, Illinois.

3. Evans, F.G., (1967) Bibliography on the Physical Properties of the Skeletal System. Artificial Limbs, Vol. 11, No. 2, pp. 48-66.

4. Frost, H.M., (1967) An Introduction to Biomechanics. Ed. C.R. Lam, Charles C. Thomas, Illinois.

5. Hudson, R.G., (1917) The Engineers' Manual, John Wiley & Sons, New York.

6. Mason, W.E., Herrmann, L.R., (1967) Elastic Analysis of Irregular Shaped Prismatic Beams by the Method of Finite Elements. Dept. of Civil Engineering, University of California, Davis, Technical Report No. 67-1.

7. Roberts, S.B., Chen, P.H. (1970) Elastostatic Analysis of the Human Thoracic Skeleton. ASME Paper 70-BHF-2.

8. Shanley, F.R., (1957) Strength of Materials. McGraw-Hill, New York.